Radiology

Effect of Radiofrequency Transmit Field Correction on Quantitative Dynamic Contrast-enhanced MR Imaging of the Breast at 3.0 T[1]

Reem Bedair, MD
Martin J. Graves, PhD
Andrew J. Patterson, PhD
Mary A. McLean, PhD
Roido Manavaki, PhD
Tess Wallace, MEng, MRes
Scott Reid, PhD
Iosif Mendichovszky, FRCR
John Griffiths, MD, DPhil
Fiona J. Gilbert, FRCR, FRCP

Purpose: To investigate the effects of radiofrequency transmit field (B_1^+) correction on *(a)* the measured T1 relaxation times of normal breast tissue and malignant lesions and *(b)* the pharmacokinetically derived parameters of malignant breast lesions at 3 T.

Materials and Methods: Ethics approval and informed consent were obtained. Between May 2013 and January 2014, 30 women (median age, 58 years; range, 32–83 years) with invasive ductal carcinoma of at least 10 mm were recruited to undergo dynamic contrast material–enhanced magnetic resonance (MR) imaging before surgery. B_1^+ and T1 mapping sequences were performed to determine the effect of B_1^+ correction on the native tissue relaxation time ($T1_0$) of fat, parenchyma, and malignant lesions in both breasts. Pharmacokinetic parameters were calculated before and after correction for B_1^+ variations. Results were correlated with histologic grade by using the Kruskal-Wallis test.

Results: Measurements showed a mean 37% flip angle difference between the right and left breast, which resulted in a 61% $T1_0$ difference in fat and a 41.5% difference in parenchyma between the two breasts. The T1 of lesions in the right breast increased by 58%, whereas that of lesions in the left breast decreased by 30% after B_1^+ correction. The whole-tumor transendothelial permeability across the vascular compartment(K^{trans}) of lesions in the right breast decreased by 41%, and that of lesions in the left breast increased by 46% after correction. A systematic increase in K^{trans} was observed, with significant differences found across the histologic grades ($P < .001$). The effect size of B_1^+ correction on K^{trans} calculation was large for lesions in the right breast and moderate for lesions in the left breast (Cohen effect size, $d = 0.86$ and $d = 0.59$, respectively).

Conclusion: B_1^+ correction demonstrates a substantial effect on the results of quantitative dynamic contrast-enhanced analysis of breast tissue at 3 T, which propagates into the pharmacokinetic analysis of tumors that is dependent on whether the tumor is located in the right or left breast.

[1] From the Department of Radiology, School of Clinical Medicine, University of Cambridge, Box 218, Cambridge Biomedical Campus, Hills Road, Cambridge CB2 0QQ, England (R.B., M.J.G., R.M., T.W., I.M., F.J.G.); Department of Radiology, Addenbrooke's Hospital, Cambridge University Hospitals NHS Foundation Trust, Hills Road, Cambridge, England (M.J.G., A.J.P., M.A.M.); Cancer Research UK Cambridge Institute, University of Cambridge, Li Ka Shing Centre, Cambridge, England (M.A.M., J.G.); and General Electric Company, GE Medical Systems Limited, Chalfont St Giles, England (S.R.). Received April 18, 2015; revision requested June 26; revision received July 30; accepted August 6; final version accepted August 18. The NIHR Biomedical Research Centre (BRC) and the Experimental Cancer Medicine Centre (ECMC) Networks funded the imaging examinations. **Address correspondence to** F.J.G. (e-mail: *fjg28@medscl.cam.ac.uk*).

Recent developments in dynamic contrast material–enhanced (DCE) magnetic resonance (MR) imaging have allowed the functional properties of tumor vascularity to be studied in vivo (1). Several studies have been conducted to investigate the diagnostic capability of DCE MR imaging in the characterization of breast lesions at 3.0 T, as the increased signal-to-noise ratio can be translated into improved spatial resolution (2,3). The application of parallel imaging techniques, together with k-space data-sharing methods, allows for improved temporal resolution, which enables quantitative pharmacokinetic (PK) modeling of contrast agent uptake (4). On implementation of PK modeling, parametric information relating to the transendothelial permeability across the vascular compartment (K^{trans}), the fractional tissue volume of interstitial space (v_e), and the rate of exchange back to the vasculature, or k_{ep}, can be derived (5).

Advances in Knowledge

- Significant differences were observed in the native tissue relaxation time ($T1_0$) of right breast fat, right parenchyma, left breast fat, and left parenchyma before and after radiofrequency transmit field (B_1^+) correction ($P < .001$ for all).
- The estimated difference in $T1_0$ between lesions in the left and right breasts was reduced from 57% to 2.5% after correction.
- A significant increase in tumor vascular permeability and/or perfusion was observed with increasing tumor aggressiveness after B_1^+ correction ($P < .001$), as lesions in the right breast exhibited lower transendothelial permeability across the vascular compartment (K^{trans}) for all grades, while lesions in the left breast exhibited higher K^{trans}.
- The effect size of B_1^+ correction on K^{trans} was large to moderate (Cohen effect size, $d = 0.86$ and $d = 0.59$ for lesions in the right and left breasts, respectively).

PK analysis has been reported to yield higher K^{trans} and k_{ep} values in breast tumors when compared with benign and normal breast tissues (6,7). Koo et al found that tumors with higher K^{trans} and k_{ep} values together with lower v_e values at 1.5 T were associated with poor prognosis and often represented the "triple-negative" cancers (estrogen receptor negative, progesterone receptor negative, and human epidermal growth factor receptor 2 negative) (8). El Khouli et al also investigated the incremental value of PK modeling in characterizing breast lesions at 3 T. They showed a similar improvement in diagnostic performance when used in conjunction with the morphologic assessment of breast lesions (3).

In other studies, investigators applied quantitative DCE MR imaging in monitoring the therapeutic response of patients undergoing neoadjuvant chemotherapy. Changes in K^{trans} have been investigated as early predictive markers of outcome at 1.5- and 3-T field strengths (9–12). Li et al (13) found that early changes in PK parameters could be used to predict the final treatment response, whereas Manton et al found that the change in lesion size was a better indicator of response (14). Given the variety of breast tumors studied and the range of acquisition protocols used, these contradictory results are not surprising.

One major challenge in the use of quantitative DCE MR imaging at 3 T is the nonuniformity of the radiofrequency transmit field (B_1^+) observed across the breasts (15). This causes right-to-left variation in the flip angle, which results in regional signal intensity increase and/or decrease. To date, only a few investigators have addressed the effect of B_1^+ variation in DCE MR imaging of the breast. Kuhl et al reported a right-left signal intensity difference in breast lesions by a factor of two at 3 T (16). This effect has been reported at 1.5 T, although to a lesser extent (17).

Numerous approaches have been proposed to mitigate the B_1^+ nonuniformity effect. These include specially designed volume coils (18) and the use of B_1^+-insensitive adiabatic pulses (19). In a recent study, investigators also described the application of active radiofrequency shimming technologies by using multichannel transmission that can reduce the signal intensity variability of the tissues across the breasts (20). However, these approaches require special hardware and can be vendor specific.

Alternatively, B_1^+ mapping methods have been used to measure the spatial variation in flip angle across the field of view. This becomes particularly relevant to PK analysis when calculating the native T1 values of tissues on conversion of signal intensity to gadolinium

Implications for Patient Care

- Because of its substantial effect, it is imperative to account for B_1^+ inhomogeneity when moving toward a standardized diagnostic MR imaging protocol at 3 T.
- Changes in K^{trans} can provide independent information regarding tumor perfusion; however, parameters should be corrected for B_1^+ nonuniformity when used as a quantitative biomarker for prediction of treatment response.

Published online before print
10.1148/radiol.2015150920 **Content codes:** BR MR

Radiology 2016; 000:1–10

Abbreviations:
B_1^+ = radiofrequency transmit field
DCE = dynamic contrast material enhanced
K^{trans} = transendothelial permeability across the vascular compartment
PK = pharmacokinetic
ROI = region of interest
$T1_0$ = native tissue relaxation time
v_e = fractional tissue volume of interstitial space
VFA = variable flip angle

Author contributions:
Guarantors of integrity of entire study, R.B., F.J.G.; study concepts/study design or data acquisition or data analysis/interpretation, all authors; manuscript drafting or manuscript revision for important intellectual content, all authors; approval of final version of submitted manuscript, all authors; agrees to ensure any questions related to the work are appropriately resolved, all authors; literature research, R.B., I.M., F.J.G.; clinical studies, R.B., M.J.G., A.J.P., M.A.M., F.J.G.; experimental studies, A.J.P., S.R.; statistical analysis, R.B., A.J.P.; and manuscript editing, all authors

Conflicts of interest are listed at the end of this article.

concentration. Sung et al reported a substantial reduction in the difference between the right and left fat T1 values in the breast by using a double-angle B_1^+ mapping method (21).

In this work, we investigated the effects of B_1^+ correction on *(a)* the measured T1 relaxation times of normal breast tissue and malignant lesions and *(b)* the PK-derived parameters of malignant breast lesions at 3 T.

Materials and Methods

Patient Population

This prospective study was approved by our institutional review and ethics committees, and informed written consent was obtained from all patients prior to the MR imaging examination. Between May 2013 and January 2014, 35 women met the eligibility criterion of biopsy-confirmed invasive ductal breast carcinoma at least 10 mm in diameter. All tumors were managed surgically, and no patients had received any treatment prior to the MR examination. In premenopausal women, care was taken to schedule the MR examination within day 6 to day 16 of their menstrual cycle. Five cases were excluded because of gross visual misregistration between the DCE series and the respective native tissue relaxation time ($T1_0$) maps due to patient motion. A total of 30 patients were included in the final analysis.

Imaging Protocol

The industrial coauthor (S.R.) from GE Healthcare, Waukesha, Wis, provided pulse sequence development support only. The first and last authors (R.B., F.J.G.) had sole control of the data and the material submitted for publication.

All MR examinations were performed on a 3.0-T system (MR 750; GE Healthcare) by using an eight-channel phased-array receive-only breast coil, with subjects lying in the prone position. Three-plane localizer images, followed by axial T1- and T2-weighted fast spin-echo images, were obtained (Table 1). The total examination time was approximately 20 minutes.

Table 1

MR Image Acquisition Parameters

Parameter	VFA T1 Mapping	Bloch-Siegert Sequence	VIBRANT-TRICKS Technique
Field of view (mm)	350	350	350
Image matrix	256 × 256	128 × 128	512 × 512
Section thickness (mm)	1.4 (interpolated)	7.0	1.4 (interpolated)
Voxel or pixel size	0.6 × 0.6 × 1.4	2.7 × 2.7	0.6 × 0.6 × 1.4
Fat suppression	No	No	Spatial-spectral water excitation
Array spatial sensitivity encoding technique factor	2 (phase direction)	…	2.5 (phase direction)
Repetition time (msec)	5.3	29	7.1
Echo time (msec)	2.1	13.5	3.8
Radiofrequency excitation (degrees)	2, 3, 5, 10, 15	20	12
Bandwidth (kHz)	±62.50	±15.63	±125
No. of sections	112	44	112
Acquisition time	41 sec for each prescribed flip angle	2 min 55 sec	8 min 7 sec

Note.—VIBRANT-TRICKS = volume image breast assessment–time-resolved imaging of contrast kinetics.

$T1_0$ mapping.—To enable the calculation of $T1_0$ values, an axial three-dimensional fast spoiled gradient-echo sequence was performed by using a variable flip angle (VFA) method at 2°, 3°, 5°, 10°, and 15°.

B_1^+ mapping.—Prior to the DCE MR imaging acquisition, the B_1^+ variation was determined by using a two-dimensional Bloch-Siegert–based gradient-echo sequence (22).

DCE MR imaging acquisition.—A three-dimensional fast spoiled gradient-echo technique with k-space data sharing (volume image breast assessment–time-resolved imaging of contrast kinetics, or VIBRANT-TRICKS) (23) was used. In this acquisition, k-space is segmented into four concentric regions, with the central region sampling interleaved with the three peripheral segments. By incorporating view sharing, images with 0.68 × 0.68 × 1.4-mm spatial resolution were reconstructed.

A catheter was placed within the antecubital vein, and a dose of 0.1 mmol of gadopentetate dimeglumine (Magnevist; Bayer Schering, Berlin, Germany) per kilogram of body weight was administered at a rate of 3.0 mL/sec by using an automated injector, followed by a 25-mL saline flush. In total, five baseline volumes were acquired, followed by 43 phases of contrast-enhanced images, with a nominal temporal resolution of 10 seconds. The dynamic data were collected in 8 minutes 7 seconds.

Postacquisition Processing and Image Analysis

MR images were reviewed on the diagnostic workstation by two radiologists (R.B. and F.J.G., with 3 and 20 years of experience in MR breast imaging, respectively). The two reviewers identified the lesions of interest in consensus. The quantitative analysis was subsequently performed by one radiologist (R.B).

B_1^+ correction maps were calculated from the Bloch-Siegert images by using in-house code written in Matlab (Mathworks, Natick, Mass), which included smoothing by using a 3 × 3 median filter. The resultant correction maps were saved as Digital Imaging and Communications in Medicine images. The VFA images, B_1^+ maps, and DCE series were processed in OsiriX (version 5.9; *www.osirix-viewer.com*), an open-source image viewer and software application. By using the DCETool plug-in (version 2.3; *http://kyungs.bol.ucla.edu/software/DCE_tool/DCE_tool.html*) (24), we calculated the native $T1_0$ maps first without

Figure 1

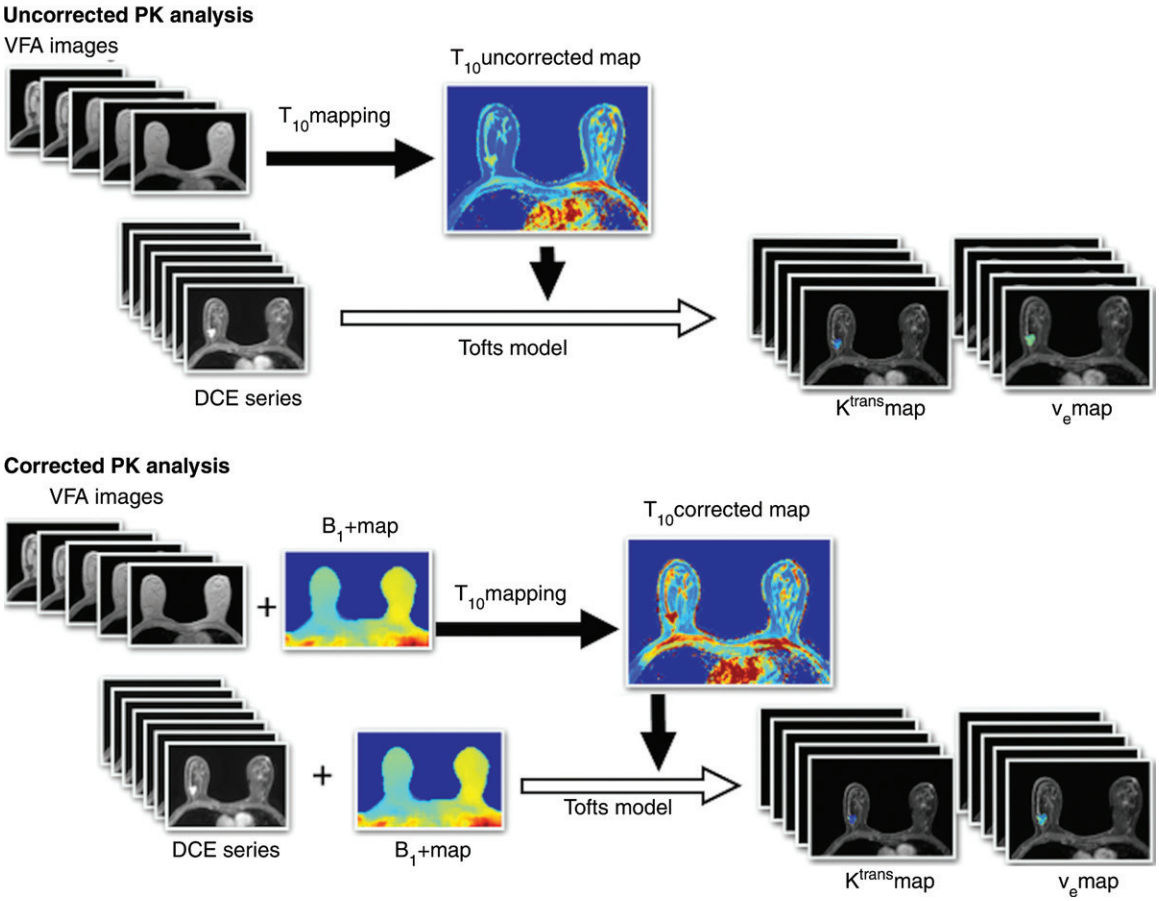

Figure 1: Diagram of the method of PK analysis at 3 T. The VFA images at 2°, 3°, 5°, 10°, and 15° are computed to generate a $T1_0$ map uncorrected for B_1^+ variation *(T_{10}uncorrected map).* This is subsequently incorporated into the PK analysis to generate parametric maps uncorrected for B_1^+. The B_1^+ map is applied to the VFA images, and a $T1_0$ corrected map *(T_{10}corrected map)* is produced. The correction is also applied to the dynamic series to generate parametric maps corrected for B_1^+.

B_1^+ correction and then after B_1^+ correction. Both $T1_0$ maps and B_1^+ maps were resampled to a matrix of 512 × 512 to match the dynamic data for the subsequent PK analysis.

As described by Azlan et al, a region of interest (ROI) that covered two-thirds of the breast was drawn on the corresponding B_1^+ map to calculate the mean flip angle variation across our cohort (25). The radiologists manually defined ROIs by encompassing the fat and parenchyma in the right and left breasts of each patient on the uncorrected and corrected $T1_0$ maps. ROIs were kept constant and were placed on matched portions of each breast to quantitatively compare T1 values in both breasts before and after B_1^+ correction. For malignant lesions, representative ROIs from the central section were drawn on the maximally enhancing DCE images and copied to both the uncorrected and corrected $T1_0$ maps to estimate $T1_0$ tumor values before and after B_1^+ correction.

Quantitative Analysis

ROIs were manually drawn on all consecutive contrast-enhanced sections of the tumor in the axial plane on the DCE MR images. Care was taken to avoid normal breast parenchyma, fat, and necrotic areas. The DCETool plug-in (source) was used to perform PK analysis by converting signal intensities of the T1-weighted DCE MR imaging data into gadolinium concentration. The two-compartmental model of Tofts et al (26) was used with a pooled arterial input function based on the modified model of Fritz-Hansen et al (27).

Both native T1 maps (uncorrected and corrected $T1_0$ maps) were used separately in the quantitative analysis. The correction maps were also applied to the DCE series to compensate for the B_1^+ variation in the dynamic sequence and were compared with that without correction. The enhancement from each voxel was measured throughout the time course of data acquisition, and the parametric color maps of K^{trans} and v_e were derived accordingly to assess

Table 2

Baseline Characteristics of the 30 Patients

Characteristic	Lesions in the Right Breast	Lesions in the Left Breast
Lesion		
Breast side	16	14
Menopausal status		
Pre- or perimenopausal	5	3
Postmenopausal	11	11
Clinical T stage		
T1	5	6
T2	9	6
T3	2	2
Tumor size at MR imaging (cm)		
<2	9	8
2–5	7	5
>5	0	1
Histologic grade		
Grade I	2	3
Grade II	7	2
Grade III	7	9
Clinical N stage		
Positive	2	2
Negative	14	12
Estrogen receptor status		
Positive	14	12
Negative	2	2
Human epidermal growth factor receptor status		
Positive	1	1
Negative	15	13

the effect of B_1^+ correction (Fig 1). Analysis was performed on K^{trans} maps with a threshold that ranged from 0.001 to 5.0 min^{-1}. Pixels with values lower than 0.001 were assumed to represent necrotic areas, while values above 5.0 min^{-1} were considered to be uncertain physiological correlates (12). An upper limit of 1.0 was imposed on v_e (5,26). For every case, the mean K^{trans} of each ROI was derived and averaged across the whole tumor to calculate whole-tumor K^{trans} values. Similarly, whole-tumor v_e values were also derived.

Histopathologic Analysis

All patients underwent surgery within a mean of 10 days after the MR examination (range, 3–17 days). Histopathologic information, including tumor size, histologic subtype, grade, and expressional status of estrogen receptors and human epidermal growth factor receptor 2 staining, were obtained from the histopathologic reports. The distribution of patients according to these prognostic factors is given in Table 2.

Statistical Analysis

The nonparametric Wilcoxon signed rank test was used for comparing the right and left breast B_1^+-corrected and uncorrected maps for fat and parenchyma. The malignant lesions in the right and left breasts were also compared before and after B_1^+ correction. All results were reported as means ± standard deviations. Cohen *d* effect sizes, computed as the mean difference between the corrected and uncorrected groups divided by the pooled standard deviations, were calculated to estimate the effect size of B_1^+ correction. Similarly, the effect of B_1^+ correction on the PK parameters according to whether the tumor was located in the left or right breast was compared. Medians, 25th and 75th percentiles, and percentages were reported, as appropriate. Group comparisons for the change in K^{trans} according to histologic tumor grade were also made by using the nonparametric Kruskal-Wallis test. Statistical significance was defined as a *P* value of up to .05. Analyses were performed by using the statistical software platform (SPSS version 21; SPSS, Chicago, Ill).

Results

Thirty women (median age, 58 years; age range, 32–83 years) with 30 histologically proven invasive ductal breast carcinomas constituted the final study population.

Figure 2 shows a contrast-enhanced image and B_1^+ and $T1_0$ maps of a breast cancer in the right breast. The mean flip angle variation ± standard deviation across our cohort was 122% ± 4.2 in the left breast and 85% ± 5.3 in the right breast. The uncorrected $T1_0$ maps show a T1 difference between the left and right breasts; however, a more uniform distribution across the breasts is observed after B_1^+ correction.

The Effect of B_1^+ Correction on $T1_0$ Values of Breast Fat, Parenchyma, and Malignant Lesions

A significant change was found between the mean $T1_0$ values of right breast fat with and without B_1^+ correction ($P < .001$). Similar significance was found between $T1_0$ of the right breast parenchyma ($P < .001$), left breast fat ($P < .001$), and left breast parenchyma ($P < .001$), as shown in Table 3 and Figure 3. The $T1_0$ difference between left and right breast fat was 61%, and this was reduced to 7% after correcting for B_1^+ nonuniformity. Similarly, the difference in parenchymal values between left and right breasts was 41.5% and was reduced to 13% after correction.

The estimated difference in $T1_0$ between malignant lesions in the left and right breasts was reduced from 57% to 2.5% after B_1^+ correction (Fig 4).

The Effect of B_1^+ Correction on PK Parameters

Given the inverse relationship between the relaxation rate and K^{trans}, lesions in the right breast demonstrated a 41% decrease in K^{trans} after correcting for B_1^+ ($P < .01$), whereas a 46% increase in K^{trans} was observed in lesions in the left breast ($P < .01$). Similarly, a significant decrease ($P < .001$) was noted in v_e of lesions in the right breast, while that of lesions in the left breast significantly increased after B_1^+ correction ($P < .001$, Table 4). Only a slight difference was observed in the spread of the distribution of PK parameters before and after correction of lesions in both breasts, as shown in Figure 5.

A systematic increase in K^{trans} was found with increasing histologic grade, with significant differences found before and after B_1^+ correction ($P < .001$, Fig 6).

The effect size of B_1^+ correction on K^{trans} was large to moderate (Cohen effect size, $d = 0.86$ and $d = 0.59$ for lesions in the right and left breasts,

Figure 2

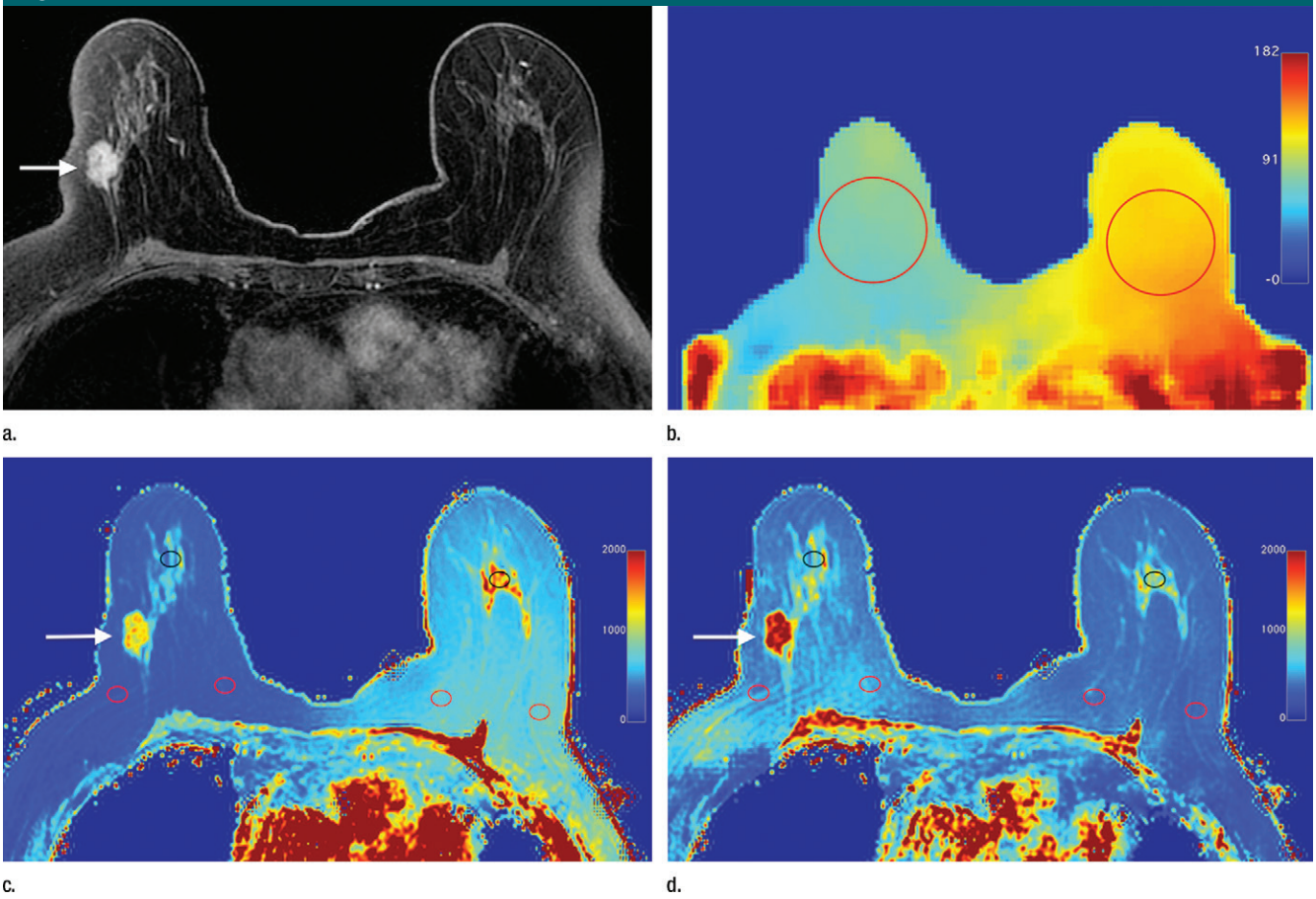

Figure 2: Representative images in a 53-year-old woman with breast cancer in the right breast. **(a)** Axial T1-weighted contrast-enhanced image of a breast cancer in the right breast (arrow) with **(b)** postprocessed B_1^+ map are shown. ROIs that cover two-thirds of the breast were drawn to estimate the flip angle variation on each side. A higher range of values is indicated in the left breast than in the right. **(c, d)** Comparison of $T1_0$ estimation before (**c**) and after (**d**) correction for B_1^+ nonuniformity. Red ROIs encompass the breast fat. Black ROIs encompass the breast parenchyma. Arrows indicate the effect of B_1^+ on the $T1_0$ of tumor.

respectively), while the effect on v_e was moderate (Cohen effect size, $d = 0.53$ and $d = 0.51$ for lesions in the right and left breasts, respectively).

Discussion

Our results demonstrate a right-to-left variation in the actual flip angle used to acquire images, which has proven to be a large source of discrepancy for measurement of the $T1_0$ values of tissues. Although we used a phase-based method of B_1^+ measurement different from that used by Sung et al, we show similar $T1_0$ measurements of fat (21). Our work also demonstrates the effect of B_1^+ correction on the $T1_0$ of parenchyma and malignant

Table 3

B_1^+ Correction Effect on $T1_0$ of Breast Tissue

Parameter	Before Correction (msec)	After Correction (msec)	Percentage Change
Fat			
Right breast	296 ± 29	464 ± 32	57% increase
Left breast	753 ± 44	435 ± 24	42% decrease
Parenchyma			
Right breast	1055 ± 194	1399 ± 272	33% increase
Left breast	1804 ± 332	1236 ± 233	31% decrease
Tumors			
Right breast	1206.2 ± 231	1902.8 ± 352	58% increase
Left breast	2797.4 ± 626	1951 ± 401	30% decrease

Note.—Unless indicated otherwise, data are means ± standard deviations.

Figure 3

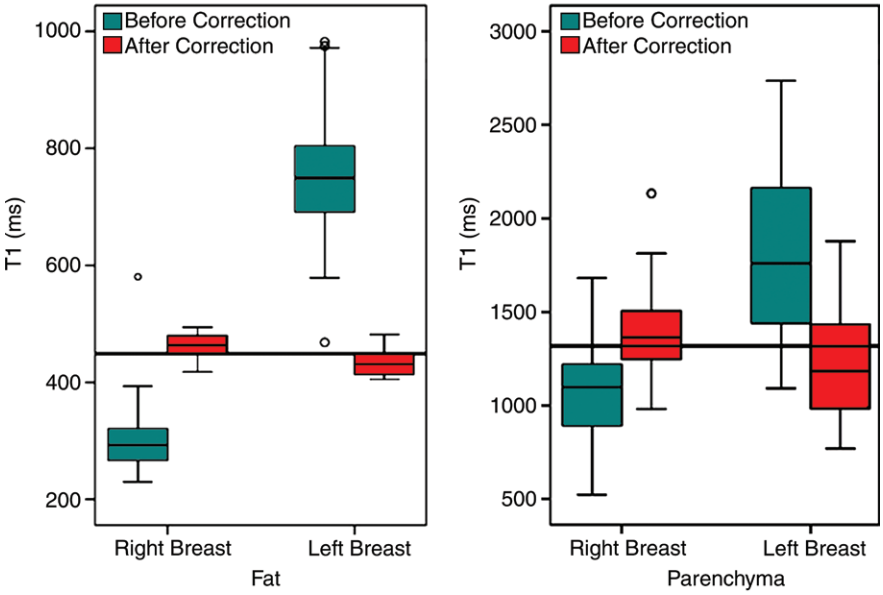

Figure 3: Box plots show the effect of B_1^+ correction on the $T1_0$ values of **(a)** fat and **(b)** parenchyma in both breasts. A significant increase is noted in the $T1_0$ of right breast fat and parenchyma after correction. The mean corrected $T1_0$ of fat for both breasts is indicated by the solid line (449 msec ± 28). Similarly, a significant decrease in the $T1_0$ of left breast fat and parenchyma is observed. The mean corrected $T1_0$ of parenchyma for both breasts is indicated by the solid line (1317.5 msec ± 252).

Figure 4

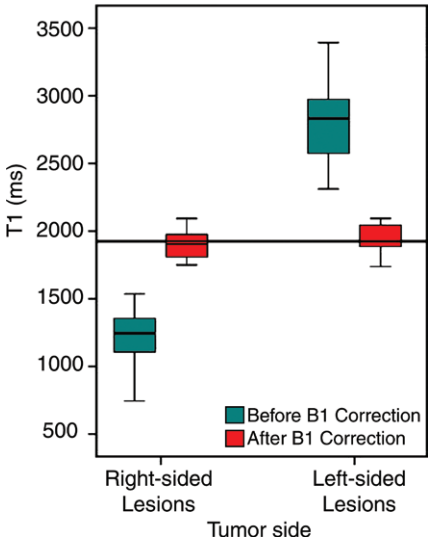

Figure 4: Box plot shows the effect of B_1^+ correction on the $T1_0$ value of lesions in the right and left breast. The estimated mean $T1_0$ across the whole population after correction was 1925 msec ± 375.

lesions. The technique, first described by Sacolick et al and improved by Turk et al, is popular, as it is robust and relatively accurate over a wide range of flip angles (22,28).

Our results demonstrate a significant change in the $T1_0$ values of fat and parenchyma when calculated for each breast separately. In the right breast, a 57% increase in the $T1_0$ value of fat and a 33% increase in the $T1_0$ value of parenchyma were found after correction. In contrast, a 42% and 31% decrease in the $T1_0$ values of fat and parenchyma, respectively, were observed in the left breast. In line with Sung et al, the T1 difference between the right and left breasts was reduced to 7% in fat and 13% in parenchyma by compensating for B_1^+ variation (21). Our resultant B_1^+-corrected $T1_0$ values are consistent with other measurements reported in the literature (29).

A similar effect was found in malignant lesions. The $T1_0$ value increased by 57.7% in lesions in the right breast, whereas the $T1_0$ of lesions in the left breast decreased by 30.2% after correction. After B_1^+ correction, the $T1_0$ difference between lesions in the right and left breast was reduced to 2.5%.

The standardization of acquisition protocols for quantitative breast imaging has been proposed to enable comparison between studies (30). In our study, we explored the effect of B_1^+ variation in the range of K^{trans} reported in the literature for breast cancer (0.05–2.20 min^{-1}) (12,31,32). Our study showed a significant decrease in PK parameters in lesions in the right breast after correction ($P < .01$). Similarly, a significant increase in values was observed for lesions in the left breast ($P < .01$). Although studies in which quantitative PK modeling was performed at 3 T had no mention of a B_1^+ correction technique for either the $T1_0$ map or the dynamic series (10,13), we found that this significantly affects the derived parameters that are dependent on whether the tumor is located in the right or the left breast.

Although our results demonstrate a smaller difference in the native $T1_0$ between the two breasts after B_1^+ correction, the difference in the lesion PK parameters may have increased after correction. This indicates that the B_1^+ field is not the sole factor that influences the disparity in K^{trans} values of lesions on both sides. We further explored the influence of histologic tumor grade on K^{trans} values. A significant increase in tumor vascular permeability and/or perfusion was observed with increasing tumor aggressiveness before and after B_1^+ correction. However, after correction, lesions in the right breast exhibited lower K^{trans} values in the range of 0.12–1.00 min^{-1} across all grades, while lesions in the left breast exhibited higher K^{trans} in the range of 0.06–2.20 min^{-1}. Further inherent tumor characteristics (eg, hormonal receptors, hypoxic status) should be investigated with regard to influence on the PK parameters, taking into consideration the B_1^+ nonuniformity.

Table 4

B_1^+ Correction Effect on PK Parameters

Parameter	Before Correction		After Correction		Percentage Change (%)
	Mean	Median	Mean	Median	
Whole-tumor K^{trans} (min^{-1})					
Lesions in the right breast	0.83 ± 0.78	0.46 (0.6–1.2)	0.49 ± 0.41	0.31 (0.2–0.7)	41% decrease
Lesions in the left breast	0.62 ± 0.69	0.39 (0.2–1.0)	0.91 ± 0.97	0.91 (0.3–1.3)	46% increase
Whole-tumor v_e					
Lesions in the right breast	0.65 ± 0.25	0.63 (0.5–0.8)	0.54 ± 0.26	0.46 (0.4–0.7)	16% decrease
Lesions in the left breast	0.50 ± 0.28	0.50 (0.4–0.6)	0.62 ± 0.26	0.63 (0.5–0.7)	23% increase

Note.—Unless indicated otherwise, values are means ± standard deviations. Numbers in parentheses are 25th–75th percentiles.

Figure 5

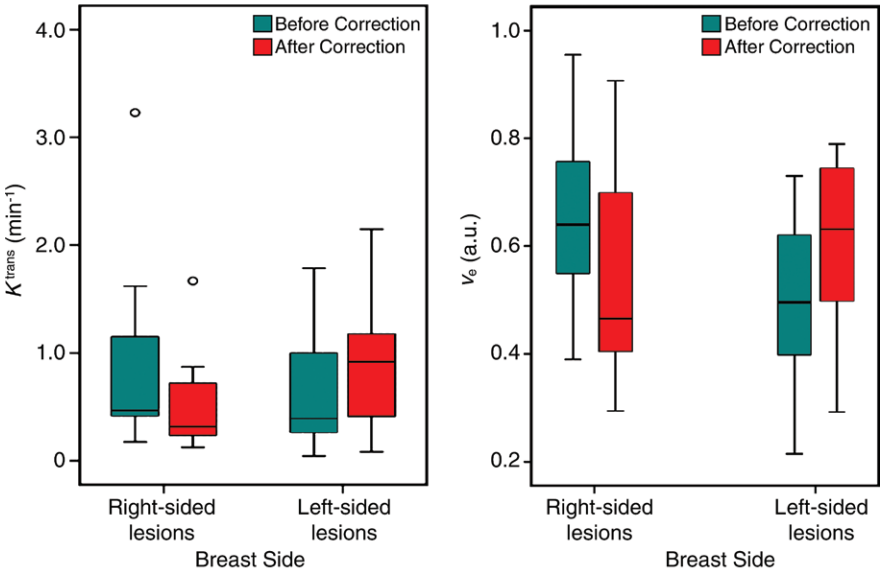

Figure 5: Box plots show the B_1^+ effect on the **(a)** K^{trans} and **(b)** v_e values of lesions in the right and left breast obtained by using whole-tumor analysis methods. Substantial decrease in lesions in the right breast is observed after correction. Conversely, a significant increase in mean K^{trans} and v_e is observed in lesions in the left breast.

Limitations of our study include inherent misalignment between the $T1_0$ maps and the images obtained with the dynamic sequence, owing to subtle patient movement. In an attempt to minimize errors, we excluded cases of gross misregistration between the $T1_0$ maps and DCE series. Further work is needed to produce optimal nonrigid image registration between the $T1_0$ and DCE series and to mitigate residual motion within the DCE series.

In our study, we did not account for the interobserver variability that could affect the measurement of the parameters, since one observer placed the ROIs.

In this study, we implemented the VFA approach, as it is the most widely used quantitative method for T1 mapping, involving the use of a three-dimensional fast spoiled gradient-echo sequence, which provides volume coverage with appropriate section resolution for subsequent pharmacokinetic analysis. At higher field strengths, however, the accuracy of the quantitative maps will be affected by inhomogeneities of the transmit field, regardless of the T1 mapping method (33). A fast B_1^+ mapping technique was used to correct the spatial variations in the nominal flip angle and minimize the systematic errors in T1 estimates.

Nonetheless, this approach continues to have a few issues. Incomplete spoiling has been identified as a potential source of error in the VFA calculation, which may in turn lead to slight overestimation of tissue relaxation (34).

There is currently no consensus on the choice of placement of the ROI within malignant lesions. In most studies, investigators have calculated K^{trans} by using the largest, most enhancing section of the lesion (8,35,36). Veltman et al and Liney et al described a hotspot method for placing the ROI within an area with the highest PK parameter values, as guided by color overlays (6,37). In our study, we implemented a whole-tumor parametric method, calculated as the multisection mean across the entire lesion. The sample size in our study is small; however, our results demonstrate a moderate to large effect size of B_1^+ correction on the PK parameters.

Our cohort included invasive ductal carcinomas only, which does not represent the range of breast neoplasms. However, invasive ductal breast carcinoma was selected to be able to study the most common type of breast cancer encountered in breast imaging clinics. Furthermore, a larger study is necessary to validate these results and study the change in K^{trans} in relation to other prognostic factors.

The variability in the results of quantitative studies has been largely attributed

Figure 6

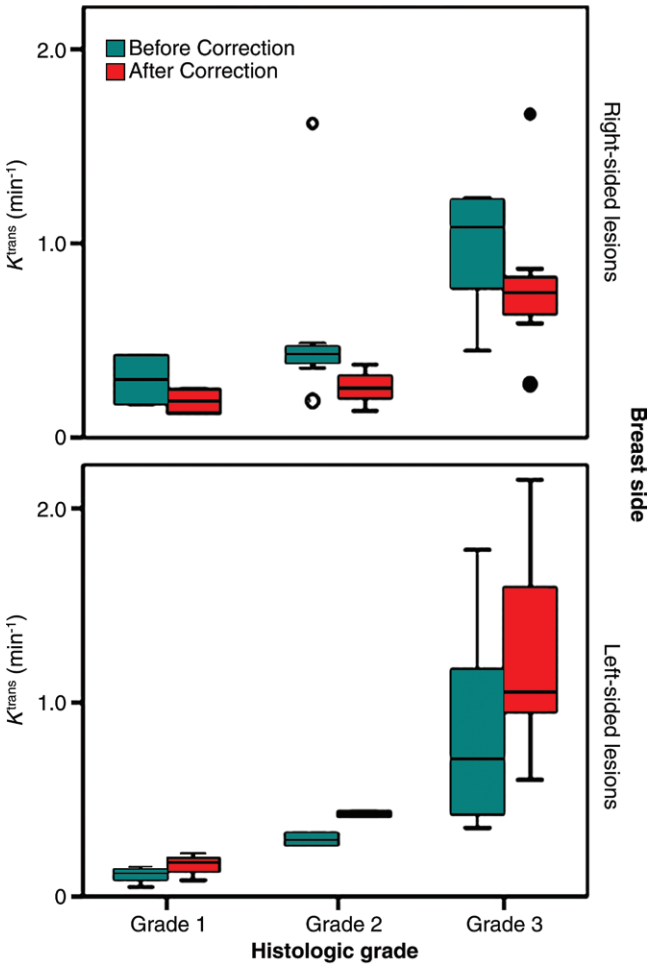

Figure 6: Box plots show the influence of histologic grade on the mean whole-tumor K^{trans} before and after correction for lesions located in the right and left breast. Significance is found between tumor grades of tumors located in the two sides, with more aggressive neoplasms exhibiting higher K^{trans} values after correction ($P < .001$).

to differences in the imaging protocol and acquisition parameters (30,32). However, the purpose of this work was to highlight the important factor of variability observed across the breasts when moving toward a standardized protocol for quantitative imaging at 3 T.

In conclusion, our work demonstrates the effect of B_1^+ nonuniformity on the relaxation properties in normal breast tissue and malignant lesions and illustrates the necessity of B_1^+ correction to prevent error propagation in subsequent PK analysis. With correction for the B_1^+ field nonuniformity, we demonstrated a substantial shift in K^{trans} and v_e that was dependent on whether the tumor was located in the right or the left breast. Although no significant change was observed in the spread of the distribution of K^{trans} across tumors after correction, a systematic increase in K^{trans} was found with increasing histologic grade, which provides independent information concerning tumor perfusion and microvascular structure.

Acknowledgments: The project was supported by the Addenbrooke's Charitable Trust and the NIHR comprehensive Biomedical Research Centre (BRC) and the Experimental Cancer Medicine Centre (ECMC) awards to Cambridge University Hospitals NHS Foundation Trust in partnership with the University of Cambridge.

Disclosures of Conflicts of Interest: R.B. disclosed no relevant relationships. **M.J.G.** disclosed no relevant relationships. **A.J.P.** disclosed no relevant relationships. **M.A.M.** disclosed no relevant relationships. **R.M.** disclosed no relevant relationships. **T.W.** disclosed no relevant relationships. **S.R.** Activities related to the present article: disclosed no relevant relationships. Activities not related to the present article: author is an employee of GE Healthcare. Other relationships: disclosed no relevant relationships. **I.M.** disclosed no relevant relationships. **J.G.** disclosed no relevant relationships. **F.J.G.** disclosed no relevant relationships.

References

1. Turnbull LW. Dynamic contrast-enhanced MRI in the diagnosis and management of breast cancer. NMR Biomed 2009;22(1):28–39.
2. Chen JH, Bahri S, Mehta RS, et al. Breast cancer: evaluation of response to neoadjuvant chemotherapy with 3.0-T MR imaging. Radiology 2011;261(3):735–743.
3. El Khouli RH, Macura KJ, Kamel IR, Jacobs MA, Bluemke DA. 3-T dynamic contrast-enhanced MRI of the breast: pharmacokinetic parameters versus conventional kinetic curve analysis. AJR Am J Roentgenol 2011; 197(6):1498–1505.
4. Planey CR, Welch EB, Xu L, et al. Temporal sampling requirements for reference region modeling of DCE-MRI data in human breast cancer. J Magn Reson Imaging 2009;30(1):121–134.
5. Sourbron SP, Buckley DL. On the scope and interpretation of the Tofts models for DCE-MRI. Magn Reson Med 2011;66(3):735–745.
6. Veltman J, Stoutjesdijk M, Mann R, et al. Contrast-enhanced magnetic resonance imaging of the breast: the value of pharmacokinetic parameters derived from fast dynamic imaging during initial enhancement in classifying lesions. Eur Radiol 2008;18(6):1123–1133.
7. Huang W, Tudorica LA, Li X, et al. Discrimination of benign and malignant breast lesions by using shutter-speed dynamic contrast-enhanced MR imaging. Radiology 2011;261(2):394–403.
8. Koo HR, Cho N, Song IC, et al. Correlation of perfusion parameters on dynamic

contrast-enhanced MRI with prognostic factors and subtypes of breast cancers. J Magn Reson Imaging 2012;36(1):145–151.

9. Pickles MD, Manton DJ, Lowry M, Turnbull LW. Prognostic value of pre-treatment DCE-MRI parameters in predicting disease free and overall survival for breast cancer patients undergoing neoadjuvant chemotherapy. Eur J Radiol 2009;71(3):498–505.
10. Jayatilake M, Li X, Tudorica A, et al. Quantitative DCE-MRI assessment of breast cancer therapeutic response: how long is the acquisition time necessary? [abstr]. In: Proceedings of the Twenty-First Meeting of the International Society for Magnetic Resonance in Medicine. Berkeley, Calif: International Society for Magnetic Resonance in Medicine, 2013.
11. Li SP, Makris A, Beresford MJ, et al. Use of dynamic contrast-enhanced MR imaging to predict survival in patients with primary breast cancer undergoing neoadjuvant chemotherapy. Radiology 2011;260(1):68–78.
12. Padhani AR, Hayes C, Assersohn L, et al. Prediction of clinicopathologic response of breast cancer to primary chemotherapy at contrast-enhanced MR imaging: initial clinical results. Radiology 2006;239(2):361–374.
13. Li X, Arlinghaus LR, Ayers GD, et al. DCE-MRI analysis methods for predicting the response of breast cancer to neoadjuvant chemotherapy: pilot study findings. Magn Reson Med 2014;71(4):1592–1602.
14. Manton DJ, Chaturvedi A, Hubbard A, et al. Neoadjuvant chemotherapy in breast cancer: early response prediction with quantitative MR imaging and spectroscopy. Br J Cancer 2006;94(3):427–435.
15. Rahbar H, Partridge SC, DeMartini WB, Thursten B, Lehman CD. Clinical and technical considerations for high quality breast MRI at 3 Tesla. J Magn Reson Imaging 2013;37(4):778–790.
16. Kuhl CK, Hendrik K, Gieseke J, Schild HH. Effect of B1 inhomogeneity on breast MR imaging at 3.0 T. Radiology 2007;244(3):939–930.
17. El Khouli RH, Thomasson D, Pang Y, Bluemke DA. Effect of B1 inhomogeneity-correction on T1-uniformity in breast MRI at 1.5 Tesla: preliminary results [abstr]. In: Proceedings of the Seventeenth Meeting of the International Society for Magnetic Resonance in Medicine. Berkeley, Calif: International Society for Magnetic Resonance in Medicine, 2009.
18. Hancu I, Lee SK, Dixon WT, et al. Field shaping arrays: a means to address shading in high field breast MRI. J Magn Reson Imaging 2012;36(4):865–872.
19. Staewen RS, Johnson AJ, Ross BD, Parrish T, Merkle H, Garwood M. 3-D FLASH imaging using a single surface coil and a new adiabatic pulse, BIR-4. Invest Radiol 1990; 25(5):559–567.
20. Rahbar H, Partridge SC, Demartini WB, Gutierrez RL, Parsian S, Lehman CD. Improved B1 homogeneity of 3 Tesla breast MRI using dual-source parallel radiofrequency excitation. J Magn Reson Imaging 2012;35(5):1222–1226.
21. Sung K, Daniel BL, Hargreaves BA. Transmit B1+ field inhomogeneity and T1 estimation errors in breast DCE-MRI at 3 Tesla. J Magn Reson Imaging 2013;38(2):454–459.
22. Sacolick LI, Wiesinger F, Hancu I, Vogel MW. B1 mapping by Bloch-Siegert shift. Magn Reson Med 2010;63(5):1315–1322.
23. Kershaw LE, Cheng HL. A general dual-bolus approach for quantitative DCE-MRI. Magn Reson Imaging 2011;29(2):160–166.
24. Sung K, Daniel BL, Rubin DL, Hargreaves B. Quantitative dynamic contrast enhanced MRI analysis tool [abstr]. In: Radiological Society of North America Scientific Assembly and Annual Meeting Program. Oak Brook, Ill: Radiological Society of North America, 2011; 315.
25. Azlan CA, Di Giovanni P, Ahearn TS, Semple SI, Gilbert FJ, Redpath TW. B1 transmission-field inhomogeneity and enhancement ratio errors in dynamic contrast-enhanced MRI (DCE-MRI) of the breast at 3T. J Magn Reson Imaging 2010;31(1):234–239.
26. Tofts PS, Brix G, Buckley DL, et al. Estimating kinetic parameters from dynamic contrast-enhanced T(1)-weighted MRI of a diffusable tracer: standardized quantities and symbols. J Magn Reson Imaging 1999;10(3):223–232.
27. Fritz-Hansen T, Rostrup E, Larsson HB, Søndergaard L, Ring P, Henriksen O. Measurement of the arterial concentration of Gd-DTPA using MRI: a step toward quantitative perfusion imaging. Magn Reson Med 1996;36(2):225–231.
28. Turk EA, Ider YZ, Ergun AS, Atalar E. Approximate Fourier domain expression for Bloch-Siegert shift. Magn Reson Med 2014 Jan 29. [Epub ahead of print]
29. Rakow-Penner R, Daniel B, Yu H, Sawyer-Glover A, Glover GH. Relaxation times of breast tissue at 1.5T and 3T measured using IDEAL. J Magn Reson Imaging 2006;23(1): 87–91.
30. Jackson A, O'Connor JP, Parker GJ, Jayson GC. Imaging tumor vascular heterogeneity and angiogenesis using dynamic contrast-enhanced magnetic resonance imaging. Clin Cancer Res 2007;13(12):3449–3459.
31. Hayes C, Padhani AR, Leach MO. Assessing changes in tumour vascular function using dynamic contrast-enhanced magnetic resonance imaging. NMR Biomed 2002;15(2): 154–163.
32. Prevos R, Smidt ML, Tjan-Heijnen VC, et al. Pre-treatment differences and early response monitoring of neoadjuvant chemotherapy in breast cancer patients using magnetic resonance imaging: a systematic review. Eur Radiol 2012;22(12):2607–2616.
33. Cheng HL, Wright GA. Rapid high-resolution T(1) mapping by variable flip angles: accurate and precise measurements in the presence of radiofrequency field inhomogeneity. Magn Reson Med 2006;55(3):566–574.
34. Yarnykh VL. Optimal radiofrequency and gradient spoiling for improved accuracy of T1 and B1 measurements using fast steady-state techniques. Magn Reson Med 2010;63(6):1610–1626.
35. Yu HJ, Chen JH, Mehta RS, Nalcioglu O, Su MY. MRI measurements of tumor size and pharmacokinetic parameters as early predictors of response in breast cancer patients undergoing neoadjuvant anthracycline chemotherapy. J Magn Reson Imaging 2007;26(3):615–623.
36. Pickles MD, Lowry M, Manton DJ, Gibbs P, Turnbull LW. Role of dynamic contrast enhanced MRI in monitoring early response of locally advanced breast cancer to neoadjuvant chemotherapy. Breast Cancer Res Treat 2005;91(1):1–10.
37. Liney GP, Gibbs P, Hayes C, Leach MO, Turnbull LW. Dynamic contrast-enhanced MRI in the differentiation of breast tumors: user-defined versus semi-automated region-of-interest analysis. J Magn Reson Imaging 1999;10(6):945–949.